

α activity of natural tungsten isotopes

F. A. Danevich, A. Sh. Georgadze, V. V. Kobychyev,* S. S. Nagorny, A. S. Nikolaiko, O. A. Ponkratenko, V. I. Tretyak, S. Yu. Zdesenko, and Yu. G. Zdesenko†
Institute for Nuclear Research, MSP 03680 Kiev, Ukraine

P. G. Bizzeti, T. F. Fazzini, and P. R. Maurenzig
Dipartimento di Fisica, Università di Firenze and INFN, I-50019 Firenze, Italy
 (Received 29 April 2002; published 22 January 2003)

The indication for the α decay of ^{180}W with a half-life $T_{1/2}^{\alpha} = 1.1_{-0.4}^{+0.8}(\text{stat}) \pm 0.3(\text{syst}) \times 10^{18}$ yr has been observed for the first time with the help of the superlow background $^{116}\text{CdWO}_4$ crystal scintillators. In a conservative approach the lower limit on half-life of ^{180}W has been established as $T_{1/2}^{\alpha}(^{180}\text{W}) \geq 0.7 \times 10^{18}$ yr at 90% C.L. In addition, new $T_{1/2}^{\alpha}$ bounds were set for α decay of ^{182}W , ^{183}W , ^{184}W , and ^{186}W at the level of 10^{20} yr.

DOI: 10.1103/PhysRevC.67.014310

PACS number(s): 23.60.+e, 29.40.Mc

I. INTRODUCTION

Alpha decay is allowed energetically for the five naturally occurring isotopes of tungsten [1], but it was never observed up to now. The α activity of tungsten with α particle energy of about 3 MeV and half-life $T_{1/2} = 2.2 \times \delta \times 10^{17}$ yr (where δ is the relative abundance of isotope) was declared in an early experiment with the nuclear emulsion technique [2]. Because the Q_{α} value for all natural tungsten nuclides, except ^{180}W , is less than 2 MeV, the result of Ref. [2] could be attributed to α decay of ^{180}W ($\delta \approx 0.12\%$ [3]) with $T_{1/2} = 2.6 \times 10^{14}$ yr. However, this observation was ruled out in the work [4], in which the cadmium tungstate (CdWO_4) crystal scintillator (mass of 20.9 g) was used as a source and detector of α decay events simultaneously. After 193 h of measurements the limit $T_{1/2} \geq 1.0 \times 10^{15}$ yr was established [4]. A similar restriction ($T_{1/2} \geq 9.0 \times 10^{14}$ yr) was also obtained in experiment (66.7 h of exposition) with ionization counter (1200 cm^2 in area) and a thin (83 $\mu\text{g}/\text{cm}^2$) sample of W (with total mass of 79 mg) enriched in ^{180}W to 6.95% [5].

These bounds were improved only recently in the measurements with two scintillators: CdWO_4 (mass of 452 g, running time of 433 h), and $^{116}\text{CdWO}_4$ enriched in ^{116}Cd to 83% (91.5 g, 951 h) [6]. The limits on the half-lives for α decay of different W isotopes were set in the range of $\approx 10^{17} - 10^{19}$ yr (see Table I).

In this paper the new results of the Kiev-Firenze experiment (2975 h of exposition) on α decay of natural tungsten isotopes are described (the preliminary analysis of the 975 h data was presented in Ref. [9]). They were obtained with the help of the superlow background spectrometer [10] based on enriched $^{116}\text{CdWO}_4$ crystal scintillators. The sensitivity of this apparatus to measure α activity was enhanced substantially in comparison with our previous work [6] mainly due

to the developed technique of pulse-shape analysis of the data, which allows us to distinguish events caused by α particles from those by γ rays (β particles).

II. EXPERIMENT AND DATA ANALYSIS**A. Experimental setup**

The setup used in our study was originally devoted to the search for the neutrinoless double beta decay of ^{116}Cd [10]. The 2β decay experiment is carried out by the Institute for Nuclear Research (Kiev)¹ in the Solotvina Underground Laboratory (allocated in a salt mine 430 m underground [11]) and results were published elsewhere [10,12]. The high purity $^{116}\text{CdWO}_4$ crystal scintillators, enriched in ^{116}Cd to 83%, were developed and grown for the search [12]. Their light output is $\approx 30\% - 35\%$ of NaI(Tl). The fluorescence peak emission is at 480 nm with principal decay time of $\approx 14 \mu\text{s}$ [13]. The CdWO_4 refractive index equals 2.3. The density of the crystal is 7.9 g/cm^3 , and the material is non-hygroscopic and chemically inert. In the apparatus (see, for details, Ref. [10]) four $^{116}\text{CdWO}_4$ crystals (total mass 330 g) are exploited. They are viewed by a low background 5 inch EMI photomultiplier tube (PMT) with a RbCs photocathode through a light guide $\varnothing 10 \times 55$ cm, which is glued with two parts: quartz (25 cm) and plastic scintillator (Bicron BC-412, 30 cm). The enriched $^{116}\text{CdWO}_4$ crystals are surrounded by an active shield made of 15 natural CdWO_4 crystals of large volume with total mass of 20.6 kg. These are viewed by a PMT through an active plastic light guide $\varnothing 17 \times 49$ cm. The whole CdWO_4 array is situated within an additional active shield made of a plastic scintillator $40 \times 40 \times 95$ cm, thus, together with both active light guides, a complete 4π active shield of the main ($^{116}\text{CdWO}_4$) detector is provided.

The outer passive shield consists of high purity copper (3–6 cm), lead (22.5–30 cm), and polyethylene (16 cm). Two plastic scintillators ($120 \times 130 \times 3$ cm) are installed

*Present address: INFN, Laboratori Nazionali del Gran Sasso, I-67010 Assergi (AQ), Italy.

†Corresponding author. Email address: zdesenko@kinr.kiev.ua

¹From 1998 by the Kiev-Firenze collaboration, Ref. [10].

TABLE I. Theoretical and experimental half-lives (or limits at 90% C.L.) for α decay of natural W isotopes obtained in the present work. The uncertainties of calculated $T_{1/2}$ values are related with uncertainties of the Q_α . The most stringent previous experimental bounds (Ref. [6]) are cited for comparison.

Isotope, abundance ^a	Q_α , MeV ^b	Calculated $T_{1/2}$, yr		Experiment $T_{1/2}$, yr	
		Based on Ref. [7]	Based on Ref. [8]	Present work	Based on Ref. [6]
¹⁸⁰ W 0.12(1)%	2.516(5)	$8.3^{+1.6}_{-1.3} \times 10^{17}$	$2.0^{+0.4}_{-0.3} \times 10^{18}$	$1.1^{+0.9}_{-0.5} \times 10^{18}$ $\geq 0.7 \times 10^{18}$	$\geq 7.4 \times 10^{16}$
¹⁸² W 26.50(16)%	1.774(3)	$3.0^{+0.5}_{-0.5} \times 10^{32}$	$1.4^{+0.3}_{-0.2} \times 10^{33}$	$\geq 1.7 \times 10^{20}$	$\geq 8.3 \times 10^{18}$
¹⁸³ W 14.31(4)%	1.682(3)		$> 5.7^{+1.3}_{-1.0} \times 10^{38}$	$\geq 0.8 \times 10^{20}$	$\geq 1.9 \times 10^{18}$
¹⁸⁴ W 30.64(2)%	1.659(3)	$3.8^{+0.9}_{-0.6} \times 10^{35}$	$2.6^{+0.6}_{-0.5} \times 10^{36}$	$\geq 1.8 \times 10^{20}$	$\geq 4.0 \times 10^{18}$
¹⁸⁶ W 28.43(19)%	1.123(7)	$8.7^{+11.2}_{-4.9} \times 10^{55}$	$2.0^{+2.6}_{-1.1} \times 10^{57}$	$\geq 1.7 \times 10^{20}$	$\geq 6.5 \times 10^{18}$

^aReference [3].

^bReference [1].

above the passive shield and are used as cosmic muon veto counters. The setup is carefully isolated against environment radon penetration. All materials for the installation were previously tested and selected for low radioactive impurities in order to reduce their contributions to background.

An event-by-event data acquisition system records the amplitude, arrival time, additional tags (the coincidence between different detectors), and pulse shape (in 2048 channels with 50 ns channel width) of the ¹¹⁶CdWO₄ detector in the energy range 0.08–5 MeV.

The energy scale and resolution of the spectrometer were determined with the γ sources ²²Na, ⁴⁰K, ⁶⁰Co, ¹³⁷Cs, ²⁰⁷Bi, ²²⁶Ra, ²³²Th, and ²⁴¹Am. The energy dependence of the resolution in the energy interval 60–2615 keV is expressed as follows: full width at half maximum (FWHM) _{γ} = $-44 + \sqrt{2800 + 23.4 \cdot E_\gamma}$, where energy E_γ and FWHM _{γ} are in keV. For instance, energy resolutions of 33.7%, 13.5%, 11.5%, and 8.0% were measured for γ lines with the energies of 60, 662, 1064, and 2615 keV, respectively. The routine calibration was carried out with ²⁰⁷Bi (weekly) and ²³²Th (monthly) γ sources. The dead time of the spectrometer and data acquisition was permanently controlled with the help of a light emitting diode optically connected to the main PMT (typical value was about 14%).

Due to active and passive shields, and as a result of the time-amplitude [10] and pulse-shape analysis of the data [13], the background rate of ¹¹⁶CdWO₄ detectors in the energy region 2.5–3.2 MeV (the $0\nu 2\beta$ decay energy of ¹¹⁶Cd is 2.8 MeV) was reduced to 0.04 counts/yr kg keV. It is the lowest background that has ever been reached with crystal scintillators.

B. Response of the ¹¹⁶CdWO₄ detector to α particles

It is well known that the relative ratio of the CdWO₄ scintillation light output for α and β particles with the same

energies (the so-called α/β ratio²) depends on the energy of the absorbed particles [6]. Because we are looking for the α decay of W isotopes, such a dependence must be precisely measured in the α energy range of 1–3 MeV (see Table I). Unfortunately, among nuclides from U/Th families there are no α emitters with such energies (the lowest available α energy is 4.0 MeV from ²³²Th). To overcome this problem, a special method of calibration was developed, in which a collimated beam of α particles from the ²⁴¹Am source was passed through a thin absorber with known thickness, thus the energy of α particles after absorber can be calculated precisely. Furthermore, it was measured with the help of a surface-barrier semiconductor detector. The dimensions of the collimator are $\varnothing 0.75 \times 2$ mm, and the thickness of a single mylar film absorber is 0.65 mg/cm². By using this technique and different sets of absorbers, α particles with energies of 0.46, 2.07, 3.04, 3.88, 4.58, and 5.25 MeV were obtained, which allows us to calibrate our detector in the energy range of interest.

It is also known that the light output of crystal scintillators may depend on the direction of α irradiation relative to the crystal axes [14]. To study this effect for CdWO₄, ¹¹⁶CdWO₄, and CaWO₄ crystals, they were irradiated by α particles in three directions perpendicular to the (010), (001), and (100) crystal planes,³ and three experimental dependencies of the α/β ratio (corresponding to three

²The detector energy scale is measured with γ sources, thus the notation “ α/γ ratio” could be more adequate. However, because γ rays interact with matter by means of the energy transfer to electrons, in the present paper we are using the traditional notation “ α/β ratio.”

³In the ¹¹⁶CdWO₄ crystal the (010) plane is perpendicular to the cylinder axis, so for the (010) direction the α source was placed on the top of crystal (in the center of the flat circle surface). For the (001) and (100) directions crystal was irradiated in the middle of the cylindrical surface.

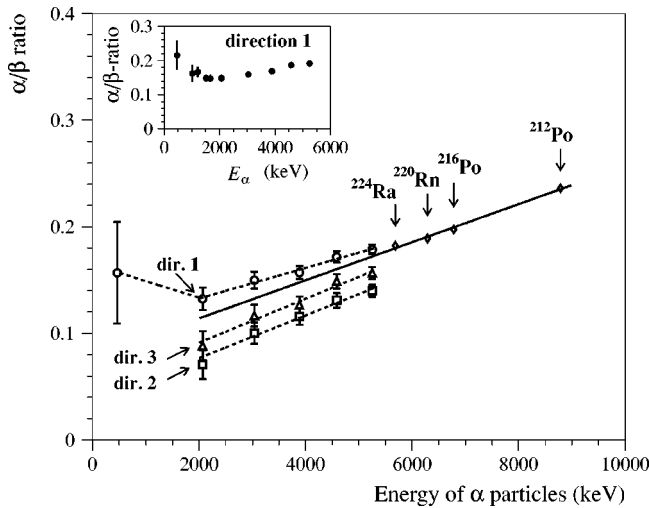


FIG. 1. The dependence of the α/β ratio on energy and direction of incident α particles measured with the enriched $^{116}\text{CdWO}_4$ scintillator ($\varnothing 32 \times 19$ mm). The crystal was irradiated by an external α source in directions perpendicular to (010), (001), and (100) crystal planes (directions 1, 2, and 3, respectively). In addition, internal α peaks of ^{224}Ra , ^{220}Rn , ^{216}Po , and ^{212}Po from the intrinsic contamination of the $^{116}\text{CdWO}_4$ crystal were used (see text). Solid lines represent the fit of the α/β ratio dependence. In the inset the behavior of the α/β ratio measured with CdWO_4 scintillator ($\varnothing 25 \times 0.9$ mm) in direction 1 is shown.

mentioned directions) as a function of α particle energy were derived from measurements. However, in a real crystal the amplitude of a light signal depends also on the point from which scintillation light is emitted (so-called nonuniformity of light collection). The latter can distort the anticipated effect of the crystal's orientation, and hence, should be properly taken into account. With this aim, the light propagation in the CaWO_4 scintillator, for which the effect of crystal orientation was not observed, was simulated with the help of the GEANT3.21 package [15] for the light emitting points on the top and side surfaces of the crystals (with dimensions $20 \times 20 \times 11$ and $40 \times 34 \times 23$ mm), as well as for those uniformly distributed inside the crystal. It was found that results of simulations are in good agreement with experiment. Then, the same simulations were performed for the $^{116}\text{CdWO}_4$ crystal ($\varnothing 32 \times 19$ mm), and results of each calibration measurement with this crystal were corrected by using simulated distributions of the light collection for α particles emitted from the corresponding point. So, values of the α/β ratio for direction 1 was multiplied by a factor of 0.85, while for directions 2 and 3, by a factor of 1.08. As an example, such corrected dependencies of the α/β ratio versus the energy and direction of α particles are shown in Fig. 1 for an enriched $^{116}\text{CdWO}_4$ crystal ($\varnothing 32 \times 19$ mm).

In addition to the measurements with the external source, the α peaks from the intrinsic trace contamination of the $^{116}\text{CdWO}_4$ crystals by nuclides from the Th chain were also used for determination of the α/β ratio. These peaks were selected from the background by using the time-amplitude analysis [10,16]. For instance, the following sequence of α decays from the ^{232}Th family was searched for and observed:

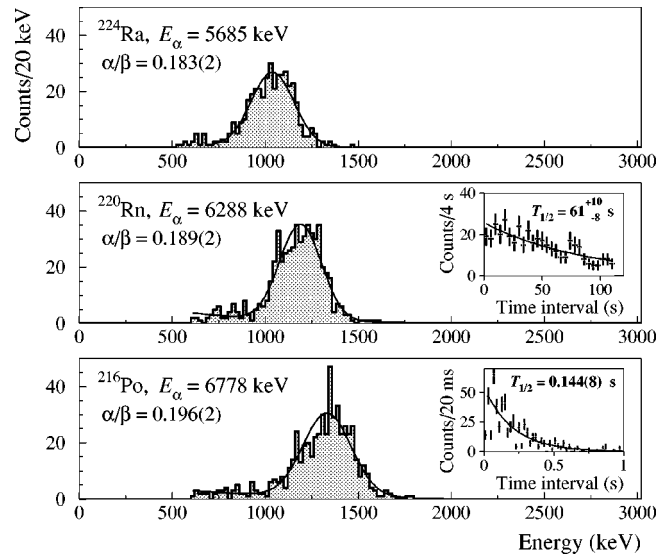


FIG. 2. The α peaks of ^{224}Ra , ^{220}Rn , and ^{216}Po selected by the time-amplitude analysis from background data accumulated during 14 745 h with the $^{116}\text{CdWO}_4$ detector. In the insets the time distributions between the first and second (and between the second and third) events together with exponential fits are presented. Obtained half-lives of ^{220}Rn and ^{216}Po [61^{+10}_{-8} s and $0.144(8)$ s, respectively] are in good agreement with the table values: $55.6(1)$ s and $0.145(2)$ s (Ref. [21]).

^{224}Ra ($Q_\alpha = 5.79$ MeV, $T_{1/2} = 3.66$ d) \rightarrow ^{220}Rn ($Q_\alpha = 6.40$ MeV, $T_{1/2} = 55.6$ s) \rightarrow ^{216}Po ($Q_\alpha = 6.91$ MeV, $T_{1/2} = 0.145$ s) \rightarrow ^{212}Pb . The obtained α peaks (the α nature of events was confirmed by a pulse-shape analysis described below), as well as the distributions of the time intervals between events, are in good agreement with those expected for α particles of ^{224}Ra , ^{220}Rn , and ^{216}Po (see Fig. 2). On this basis the activity of ^{228}Th in $^{116}\text{CdWO}_4$ crystals was determined as $39(2)$ $\mu\text{Bq/kg}$.⁴ Moreover, the α peak of ^{212}Po (the daughter of ^{212}Bi) was reconstructed with the help of the front edge analysis of the scintillation signals. The energy and time distributions of the sequence of β decay of ^{212}Bi and α decay of ^{212}Po , selected from the background, are presented in Figs. 3(a)–3(c), while a typical example of such an event is shown in Fig. 3(d).

The values of the α/β ratio, derived with the internal α peaks, and their fit are depicted in Fig. 1. Fit yields for the energy range 2.0–8.8 MeV are $\alpha/\beta = 0.083(9) + 0.0168(13) \cdot E_\alpha$, where E_α is in MeV.⁵ Because in measurements with internal sources the effect of the crystal's orientation is averaged, such an extrapolation of the fit into the energy region 2.0–5.5 MeV is reasonable and it was also proved by the behavior of the α/β ratios measured

⁴The same technique was applied to the sequence of decays from the ^{235}U and ^{238}U families. Activity of $5.5(14)$ $\mu\text{Bq/kg}$ for ^{227}Ac (^{235}U family) and the limit ≤ 5 $\mu\text{Bq/kg}$ for ^{226}Ra (^{238}U family) in the $^{116}\text{CdWO}_4$ crystals were set.

⁵The growth of the α/β ratio with α particles energy has been earlier observed for cadmium tungstate (Ref. [6]) and other scintillators (Refs. [14,16,17].)

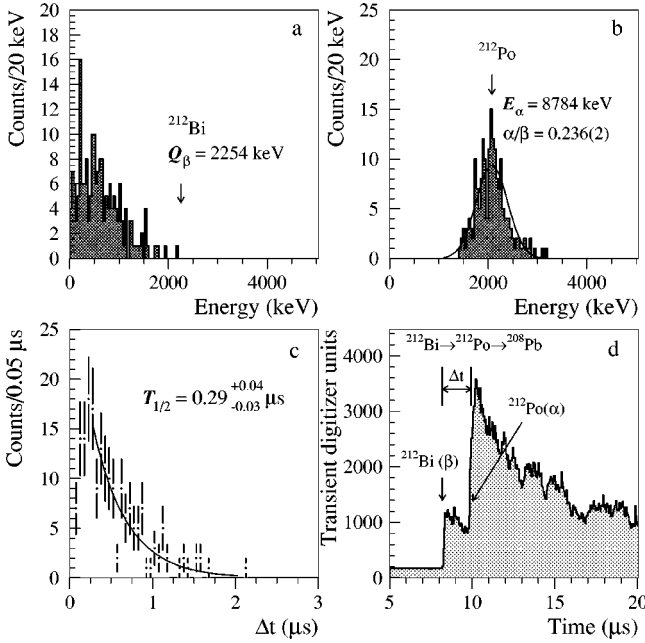


FIG. 3. The energy (a) and (b) and time (c) distributions for the fast sequence of β (^{212}Bi , $Q_\beta = 2254$ keV) and α [^{212}Po , $E_\alpha = 8784$ keV, $T_{1/2} = 0.299(2)$ μs] decays selected from the background data by the pulse-shape analysis. (d) Example of such an event in the $^{116}\text{CdWO}_4$ scintillator.

with external sources (see Fig. 1). At the same time, in the α energy interval of 0.5–2.0 MeV we find that the α/β ratio is decreased with the energy. It was also confirmed by the measurement with the thin ($\varnothing 25 \times 0.9$ mm) CdWO_4 crystal scintillator (see inset in Fig. 1). Similar behavior (a fall with energy in the 10–100 keV energy region) of relative scintillation efficiency for Ca and F recoil nuclei in the $\text{CaF}_2(\text{Eu})$ scintillator was reported in Ref. [18]. Thus, for the 0.5–2.0 MeV energy range we obtain $\alpha/\beta = 0.15(3) - 0.015(8) \cdot E_\alpha$, where E_α is in MeV.

The calibration data were also used to determine the energy resolution of the detector for α particles: $\text{FWHM}_\alpha(\text{keV}) = 33 + 0.247E_\alpha^\gamma$, where E_α^γ is the energy of α particles in the γ scale expressed in keV.

C. Pulse-shape analysis

The pulse-shape analysis of CdWO_4 scintillation signals was developed on the basis of the optimal digital filter [19], and clear discrimination between γ rays (electrons⁶) and α particles was achieved [13]. The pulse shape of cadmium tungstate scintillators can be described as $f(t) = \sum A_i / (\tau_i - \tau_0) \cdot (e^{-t/\tau_i} - e^{-t/\tau_0})$, where A_i are amplitudes and τ_i are decay constants for different light emission components, and τ_0 is the integration constant of electronics (≈ 0.18 μs). To provide an analytic description of the α or γ signals, the

⁶Because γ rays interact with matter by means of the energy transfer to electrons, it was assumed and experimentally proved with β particles from the decay of internal ^{113}Cd that pulse shapes for electrons and γ 's are the same.

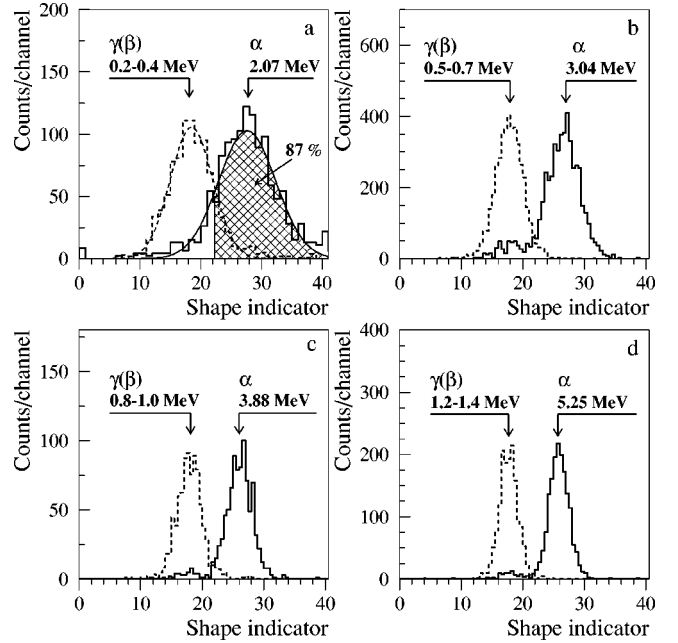


FIG. 4. Examples of the shape indicator distributions measured by the enriched $^{116}\text{CdWO}_4$ crystal scintillator ($\varnothing 32 \times 19$ mm) with α particles and γ rays with different energies: (a) $E_\gamma = 0.2\text{--}0.4$ MeV, $E_\alpha = 2.07$ MeV; (b) $E_\gamma = 0.5\text{--}0.7$ MeV, $E_\alpha = 3.04$ MeV; (c) $E_\gamma = 0.8\text{--}1.0$ MeV, $E_\alpha = 3.88$ MeV; (d) $E_\gamma = 1.2\text{--}1.4$ MeV, $E_\alpha = 5.25$ MeV.

pulse shape resulting from the average of a large number of individual events has been fitted with the sum of three (for α particles) or two (for γ 's) exponents, giving the reference pulse shapes $\bar{f}_\alpha(t)$ and $\bar{f}_\gamma(t)$ (see, for details, Ref. [13]). For the enriched crystals (used in the experiment) the following values were obtained: $A_1^\alpha = 80.9$, $\tau_1^\alpha = 12.7$ μs , $A_2^\alpha = 13.4$, $\tau_2^\alpha = 3.3$ μs , $A_3^\alpha = 5.7$, and $\tau_3^\alpha = 0.96$ μs for ≈ 5 MeV α particles and $A_1^\gamma = 94.2$, $\tau_1^\gamma = 13.6$ μs , and $A_2^\gamma = 5.6$, $\tau_2^\gamma = 2.1$ μs for ≈ 1 MeV γ quanta.

In the data processing the digital filter was applied to each experimental signal $f(t)$ with an aim to obtain the numerical characteristic of its shape defined as SI (shape indicator): $SI = \sum f(t_k) \times P(t_k) / \sum f(t_k)$, where the sum is over time channels k , starting from the origin of the signal and up to 50 μs , and $f(t_k)$ is the digitized amplitude (at the time t_k) of a given signal. The weight function $P(t)$ is defined as

$$P(t) = \{\bar{f}_\alpha(t) - \bar{f}_\gamma(t)\} / \{\bar{f}_\alpha(t) + \bar{f}_\gamma(t)\}.$$

The SI distributions measured with different α and γ sources (see some examples in Fig. 4) are well described by Gaussian functions, whose standard deviations $\sigma(SI_\alpha)$ and $\sigma(SI_\gamma)$ depend on energy: $\sigma(SI_\alpha) = -0.3 + 0.7 \times 10^{-3} E_\alpha^\gamma + 1700/E_\alpha^\gamma$ for α particles, and $\sigma(SI_\gamma) = 1.51 - 0.23 \times 10^{-3} E_\gamma + 402/E_\gamma$ for γ quanta, where E_α^γ and E_γ are in keV. As is seen from Fig. 4, electrons (γ rays) and α particles are clearly distinguished for the energies above 0.6 MeV ($E_\alpha \approx 3$ MeV), while the pulse-shape discrimination ability of the CdWO_4 scintillator worsens at lower energies. Nevertheless, it is also visible from Fig. 4(a) that even 2

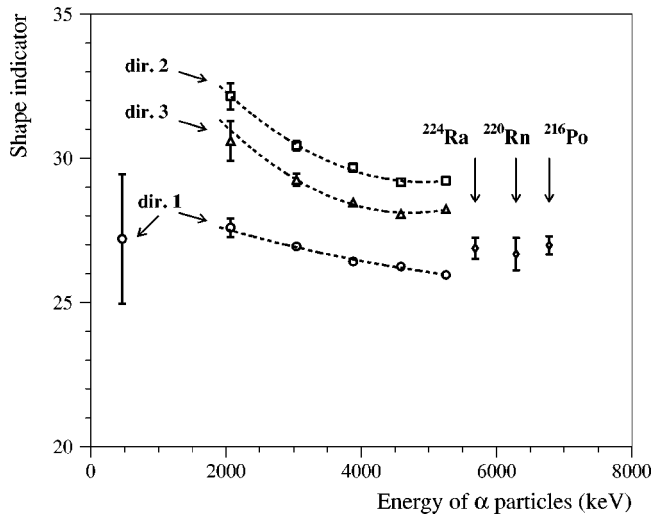


FIG. 5. The dependence of the shape indicator on the energy and the direction of incident α particles measured with the enriched $^{116}\text{CdWO}_4$ crystal scintillator. The α peaks of ^{224}Ra , ^{220}Rn , and ^{216}Po were selected by the time-amplitude analysis of background data.

MeV α particles ($E_\alpha^\gamma \approx 0.3$ MeV) can be separated from γ background with reasonable accuracy. For instance, with the requirement that $\approx 87\%$ of α particles must be registered we will get about 13% of γ events as background [see Fig. 4(a)].

The dependence of the pulse shape on energy and direction of α particles measured with the enriched $^{116}\text{CdWO}_4$ crystal scintillator ($\varnothing 32 \times 19$ mm) is presented in Fig. 5. In the energy range of 0.5–7.0 MeV the average dependence of the shape indicator on the energy can be approximated by the function $SI_\alpha = 29.5 - 0.195 \times 10^{-2} E_\alpha^\gamma$, where E_α^γ is in keV.

For γ quanta the energy dependence of the shape indicator was measured with γ sources in the energy range 0.04–3.2 MeV: $SI_\gamma = 18.4 - 0.117 \times 10^{-2} E_\gamma + 0.54 \times 10^{-6} E_\gamma^2$, where E_γ is in keV.

In addition, a digital filter for the pulses of the plastic scintillator light guide was developed and clear separation was obtained for the pure events in the plastic and cadmium tungstate scintillators. It allows us to discriminate plastic pulses in more complicated cases, when they are overlapped with the signals of $^{116}\text{CdWO}_4$ crystals. The use of this filter leads to some loss of the registration efficiency for the events in the $^{116}\text{CdWO}_4$ detector (of the order of $\approx 5\%$), which, however, can be correctly taken into account on the basis of calibration measurements.

III. RESULTS AND DISCUSSION

A. Background interpretation

The background spectra of ($\gamma + \beta$) and α events measured by four $^{116}\text{CdWO}_4$ crystals (330 g, exposition 2975 h) are depicted in Fig. 6.

The $\gamma(\beta)$ spectrum shown in Fig. 6 was built by selecting the following interval of SI values: $SI_\gamma - 2.4\sigma_\gamma < SI < SI_\gamma + 2.4\sigma_\gamma$, which contains 98% of $\gamma(\beta)$ events. In the low energy region the background of the $^{116}\text{CdWO}_4$ detector is

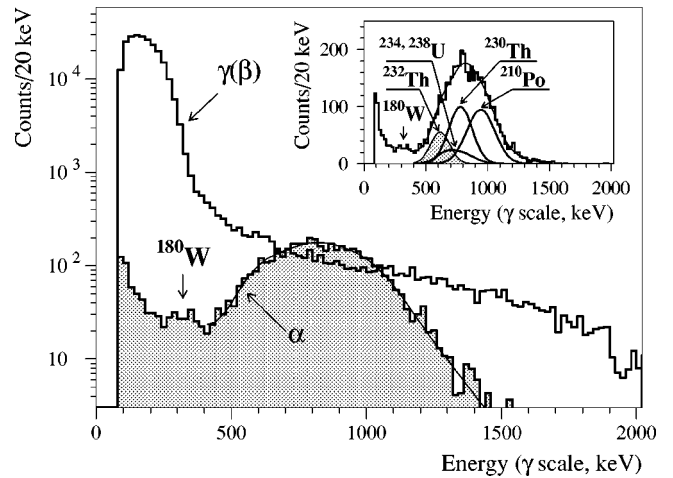


FIG. 6. Energy distributions of $\gamma(\beta)$ and α events, which were selected by the pulse-shape analysis from the data of $^{116}\text{CdWO}_4$ crystals (330 g) measured during 2975 h. In the inset, the α spectrum is depicted together with the model, which includes α decays from ^{232}Th and ^{238}U families. The total α activity in the $^{116}\text{CdWO}_4$ crystals is 1.40(10) mBq/kg.

caused mainly by the fourth-forbidden β decay of ^{113}Cd ($T_{1/2} = 7.7 \times 10^{15}$ yr [20], $Q_\beta = 316$ keV [21]) which is present in the enriched crystal with an abundance of $\delta \approx 2\%$. The distribution above ≈ 350 keV is described by a trace contamination of the enriched and shield crystals by ^{40}K , ^{137}Cs , and ^{113m}Cd , the two neutrino double beta decay of ^{116}Cd with $T_{1/2} = 2.6 \times 10^{19}$ yr [10], and external γ rays.

The energy spectrum of α particles (Fig. 6) was obtained by selection of events with the following values of the shape indicator: $SI_\gamma + 4\sigma_\gamma < SI < SI_\alpha + 2.4\sigma_\alpha$. Under such restrictions the efficiency of the pulse-shape analysis (η_{PSA}) depends on the energy of α particles. For example, for α peak of ^{180}W this efficiency equals 49.5%, while additional use of the filter for the plastic pulses discrimination decreases this value down to 47%.

Taking into account the fact that secular equilibrium in crystal scintillators is usually broken, the distribution of the α events is well reproduced by the model (see inset in Fig. 6), which includes α decays from ^{232}Th and ^{238}U families. For illustration, the results of the pulse-shape analysis of the data (for energy above 350 keV) are presented in Fig. 7 as a three-dimensional distribution of the background events versus the energy and shape indicator. In this plot one can see a clearly separated population of the α events, which belong to U/Th families. The total α activity associated with the peak in the energy region 400–1500 keV is 1.40(10) mBq/kg. However, because of a poor energy resolution for α particles and the uncertainty of the α/β ratio, we give only limits on the activity of nuclides from uranium and thorium families in the $^{116}\text{CdWO}_4$ scintillators received from the fit of the spectrum in the range 400–1500 keV: $^{232}\text{Th} \leq 0.15$ mBq/kg, ^{238}U (^{234}U) ≤ 0.6 mBq/kg, $^{230}\text{Th} \leq 0.5$ mBq/kg, and $^{210}\text{Pb} \leq 0.4$ mBq/kg.

The low energy part of the α spectrum (below 200 keV) can be explained by the PMT noise, residual $\gamma(\beta)$ background, γ or β events in the $^{116}\text{CdWO}_4$ scintillators with a

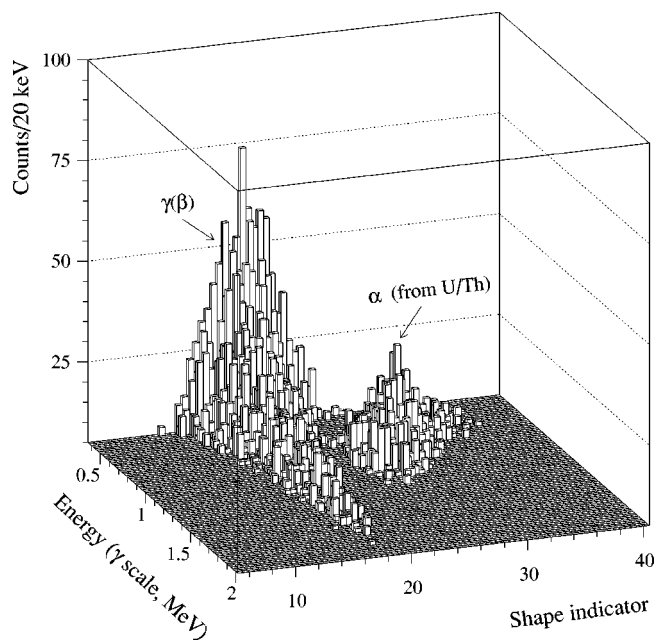


FIG. 7. Three-dimensional distribution of the background events (2975 h of exposition with the $^{116}\text{CdWO}_4$ crystals) versus energy and shape indicator. The population of α events belonging to the U/Th families is clearly separated from the $\gamma(\beta)$ background.

small admixture of the plastic light-guide pulses (which were not discriminated by the pulse-shape analysis), decays of Th and U daughter α nuclides located inside defects, or inclusions of the crystals (in that case alpha particles can lose a part of their energy without scintillation light emission), etc.

Lastly, a small peak is visible in the α spectrum of Fig. 6 at the energy around 300 keV. Since the 2.46 MeV α peak of ^{180}W is expected at 307 ± 24 keV (with FWHM = 110 keV), and because the position of the α peak of ^{232}Th (with the lowest α energy of 4.0 MeV among all α emitters from U/Th families) must be at ≈ 600 keV, it is unlikely that this small peak can be attributed to an origin other than α decay of ^{180}W . However, because a platinum crucible was used for the growth of our crystals, we analyze the possible imitation of the effect by α activity of ^{190}Pt (the abundance of ^{190}Pt is 0.014% [3], $T_{1/2} = 6.5 \times 10^{11}$ yr, $E_\alpha = 3164(15)$ keV [21], or 435 ± 30 keV in γ scale). Calculation shows that the detected peak can be caused by platinum pollution (homogeneously spread in the volume of the $^{116}\text{CdWO}_4$ scintillators) at the level of ≈ 3 ppm. To estimate the actual platinum contamination in cadmium tungstate crystals, the results of previous low background measurements performed by the Milano-Kiev collaboration with the CdWO_4 crystal⁷ of 58 g [22] were considered. This experiment has been carried out in the Gran Sasso Underground Laboratory, and the CdWO_4 crystal was used as a low temperature (≈ 25 mK) bolometer. Energy resolution (FWHM) of the detector was equal to 5 keV at 2.6 MeV. No events were registered in the energy region of 3100–3300 keV during 340 h, which allows us to set

⁷This crystal was produced in the same apparatus as the enriched ones.

bounds on the ^{190}Pt activity. In accordance with Refs. [23,24] it yields 1.3 counts as the limit for the number of events, which can be excluded with 68% C.L., hence one can set a bound for platinum concentration in the cadmium tungstate crystal to be 1.2 ppm. In addition, two samples of the CdWO_4 crystal with dimensions $1.5 \times 1.5 \times 0.1$ cm were searched (with the help of the electron microscope) for inclusions, whose elemental composition is different from that of CdWO_4 . With this aim, a flat surface (2 cm^2) of each sample was scanned, and if such an inclusion was observed, the electron beam was concentrated on it and the emitted X rays were analyzed with a crystal spectrometer (with energy resolution better than 0.1 eV) tuned on a characteristic platinum X ray. For any observed inclusions (with diameters in the range 2–30 μm) no emission of platinum X rays was found. This results in the conclusion that the limit (95% C.L.) on platinum concentration in the CdWO_4 crystal is lower than 0.1 ppm (or 0.03 ppm) for Pt inclusions with diameters less than 5 μm (or 3 μm). Similar analysis performed with the small sample (≈ 3 cm in diameter) of the enriched $^{116}\text{CdWO}_4$ crystal gives even more stringent restrictions:⁸ 0.07 ppm (or 0.02 ppm).

Therefore, one can conclude that all bounds obtained for homogeneous Pt contaminations in the CdWO_4 crystals are well below the level of 3 ppm, at which the α peak of ^{180}W could be imitated. Moreover, it is also known that in crystals that were grown in a platinum crucible, Pt is not distributed homogeneously, but it is present in the form of precipitates with a size around 20 μm [25], hence a broad energy distribution instead of an α peak would be observed. The latter was proved by our Monte Carlo simulation of the ^{190}Pt α decays in the CdWO_4 crystal with the help of the GEANT and event generator DECAY4 [26]. It suggests that the effect of ^{180}W α activity could be imitated by ^{190}Pt alpha decays only in the case of platinum particles of 2–3 μm in size, with Pt average concentration in the crystals at the level of 4–6 ppm, which is much larger than our experimental limits.

Nevertheless, because it is impossible to exclude (at least in principle) some other explanations of the 300 keV peak in the background spectrum, we can treat our experimental result only as the first indication for the possible α decay of ^{180}W . Obviously, final confirmation of its existence would be obtained with the help of CdWO_4 crystals enriched with/depleted of ^{180}W . However, it is clear that preparation and performance of such a measurement would require strong additional effort and perhaps a long time.

B. Alpha activity of ^{180}W and other tungsten isotopes

Assuming that the observed peak at the energy around 300 keV is really caused by α decay of ^{180}W , let us estimate its half-life. With this aim the experimental α spectrum in the energy region of interest was fitted by a Gaussian distribution (FWHM = 110 keV), which represents the effect, and by the background model. The latter was built up as a sum of

⁸This is due to larger scanned area and better spatial resolution of the electron microscope used in this case.

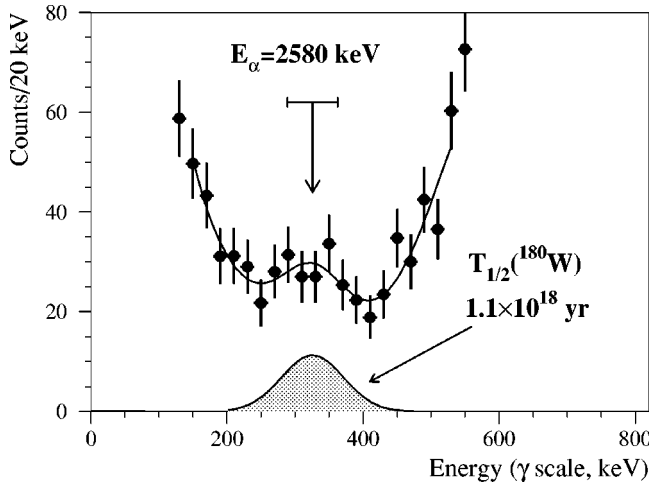


FIG. 8. Fragment of the α spectrum measured with the $^{116}\text{CdWO}_4$ detector during 2975 h together with the fitting curve (solid line). The α peak of ^{180}W with an area of 64 counts corresponds to a half-life of 1.1×10^{18} yr.

the α peak of ^{232}Th and the exponential function. Position and area of the searched peak, the thorium α peak area, and constants of the exponent were taken as free parameters of the fit procedure, which was performed in the energy region $(140 \pm 20) - (510 \pm 30)$ keV. The best fit ($\chi^2/\text{n.d.f.} = 0.52$) achieved in the interval 140–520 keV (see Fig. 8) gives the area of the searched peak $S = 64 \pm 26$ counts and its position at 326 ± 15 keV. Therefore, the measured energy of ^{180}W alpha particles is 2580 ± 290 keV, which is in a reasonable agreement with the theoretical value $E_{\alpha} = 2460$ keV. Taking into account the number of ^{180}W nuclei in the crystals (6.57×10^{20}) and the total efficiency (47%), we get the corresponding half-life value: $T_{1/2}^{\alpha}(^{180}\text{W}) = 1.1^{+0.8}_{-0.4}(\text{stat}) \pm 0.3(\text{syst}) \times 10^{18}$ yr. The systematic error is related mainly to an uncertainty of the background model.

In more conservative approach we use results of our fit in order to set the upper limit on half-life of ^{180}W : $\lim T_{1/2}^{\alpha}(^{180}\text{W}) \geq 0.7 \times 10^{18}$ yr at 90% C.L.⁹

In addition, since there are no structural features in the experimental α spectrum, which could indicate an α activity of other tungsten isotopes, half-life bounds for these processes were estimated. The numbers of candidate nuclei in the detector with a mass of 330 g are $^{182}\text{W} - 1.45 \times 10^{23}$, $^{183}\text{W} - 7.83 \times 10^{22}$, $^{184}\text{W} - 1.68 \times 10^{23}$, and $^{186}\text{W} - 1.56 \times 10^{23}$. The position of the α peak in the γ equivalent scale, the expected peak width, and the efficiency of the pulse-shape analysis are ^{182}W ($E_{\alpha}^{\gamma} = 215 \pm 57$ keV; $\text{FWHM}_{\alpha} = 86$ keV; $\eta_{\text{PSA}} = 35\%$), ^{183}W ($E_{\alpha}^{\gamma} = 206 \pm 54$ keV; $\text{FWHM}_{\alpha} = 83$ keV; $\eta_{\text{PSA}} = 34\%$), ^{184}W ($E_{\alpha}^{\gamma} = 204 \pm 53$ keV; $\text{FWHM}_{\alpha} = 83$ keV; $\eta_{\text{PSA}} = 34\%$), and ^{186}W ($E_{\alpha}^{\gamma} = 147 \pm 34$ keV; $\text{FWHM}_{\alpha} = 69$ keV; $\eta_{\text{PSA}} = 28\%$). Fitting the ex-

perimental α spectrum by a sum of the expected peak and background model (exponential function plus α peaks of ^{180}W and ^{232}Th) we get the following half-life limits (at 90% C.L.):

$$T_{1/2}(^{182}\text{W}) \geq 1.7 \times 10^{20} \text{ yr}, \quad T_{1/2}(^{183}\text{W}) \geq 0.8 \times 10^{20} \text{ yr},$$

$$T_{1/2}(^{184}\text{W}) \geq 1.8 \times 10^{20} \text{ yr}, \quad T_{1/2}(^{186}\text{W}) \geq 1.7 \times 10^{20} \text{ yr}.$$

The obtained experimental results for α activity of naturally occurring tungsten isotopes are summarized in Table I.

C. Comparison with theory

To our knowledge, there is only one theoretical work, based on the microscopic approach, in which the half-life for α decay of ^{180}W was calculated [27]. It takes into account the systematic behavior of the reduced α widths of even-even nuclei with numbers of neutrons and protons $N \geq 84$, $Z \leq 84$ and penetration factors obtained from realistic cluster wave functions. The derived result is $T_{1/2}^{\alpha} = 7.5 \times 10^{17}$ yr and uncertainty of this value is estimated to be less than a factor of 3 [27]. For other tungsten isotopes theoretical predictions are absent.

We have calculated the half-lives of all W isotopes for α decay, first, with the help of the cluster model [7], which was very successful in describing the α decays of even-even nuclei. For example, it reproduces the $T_{1/2}^{\alpha}$ values mainly within a factor of 2 for a wide range of nuclides (from $^{106}_{52}\text{Te}$ to $^{264}_{108}\text{Hs}$) and for $T_{1/2}^{\alpha}$ from 10^{-7} s to 10^{16} yr. Because α decays of natural W isotopes (except ^{183}W) occur without changes in nuclear spin and parity, we have chosen a set of 17 nuclides (from $^{144}_{60}\text{Nd}$ to $^{248}_{96}\text{Cm}$) with $T_{1/2}^{\alpha} > 10^5$ yr [28], whose α decays also proceed without changes in nuclear spin and parity. When comparing theory with experiment, it is practical to use the value of the deviation $\chi = \max(R, 1/R)$, where $R = T_{1/2}^{\text{th}}/T_{1/2}^{\text{exp}}$. For the chosen set of nuclides the cluster model [7] gives a quite reasonable average value of $\chi = 1.9$. Then, half-lives for W isotopes were calculated with the help of the cluster model [7] and obtained results are listed in Table I (given uncertainties are related only with uncertainties of Q_{α}). In particular, $T_{1/2}^{\alpha}(^{180}\text{W}) = 8.3 \times 10^{17}$ yr, which is very close to the value of 7.5×10^{17} yr derived in Ref. [27].

Semiempirical relationships are often more effective in the prediction of $T_{1/2}^{\alpha}$ than microscopically based calculations. We found in the literature [8,29–37] 18 semiempirical formulas which can be used for our purpose. All of them were also tested with the same set of 17 nuclides with $T_{1/2}^{\alpha} > 10^5$ yr. The best result (average deviation of the calculated values from experiment $\chi = 1.9$) was found for the relationship of Ref. [8] based on phenomenological fission theory of α decay and valid not only for even-even but also for odd-even, even-odd, and odd-odd nuclei. The values of $T_{1/2}^{\alpha}$ obtained in such approach for W isotopes are given in Table I, where uncertainties are caused, as in the previous case, by uncertainties of Q_{α} . For the ^{183}W decay it was also taken into account that change in parity will additionally suppress the decay rate as compared with that of Ref. [8]. For ^{180}W

⁹A similar bound $T_{1/2}^{\alpha} \geq 1 \times 10^{18}$ yr at 90% C.L. can be extracted from the mentioned measurements (340 h) with the CdWO_4 crystal of 58 g used as a low temperature bolometer (Ref. [22]), where no events were observed within the energy interval 2516 ± 30 keV.

our result $T_{1/2}^{\alpha} = 2.0 \times 10^{18}$ yr is also close to that of [27].

Thus, we can conclude that the half-life value ($T_{1/2}^{\alpha} = 1.1_{-0.5}^{+0.9} \times 10^{18}$ yr) for possible α decay of ^{180}W (the indication of which is observed in the present work) is in good agreement with the theoretical predictions: $T_{1/2}^{\alpha} = 0.75 \times 10^{18}$ yr (microscopic approach [27]), and calculated here on the basis of the semiempirical formula [8] and cluster model [7] as $T_{1/2}^{\alpha} = 2.0 \times 10^{18}$ yr and $T_{1/2}^{\alpha} = 0.83 \times 10^{18}$ yr, correspondingly.

IV. CONCLUSIONS

In the present work the pulse shape and α/β ratio of the CdWO₄ crystal scintillators have been studied for three directions of the collimated beam of α particles relatively to the main crystal axes in the energy range 0.5–5.2 MeV. The dependencies of the α/β ratio and pulse shape on the direction of α irradiation have been found and measured.

By using the superlow background $^{116}\text{CdWO}_4$ crystal scintillators, the indication for the α decay of the natural tungsten isotope ^{180}W was observed for the first time. The measured half-life $T_{1/2}^{\alpha} = 1.1_{-0.4}^{+0.8}(\text{stat}) \pm 0.3(\text{syst}) \times 10^{18}$ yr is close to the theoretical predictions, and it would be the most

rare α decay ever observed in nature. More conservatively our result can be treated as the lower limit on the half-life of ^{180}W : $\lim T_{1/2}^{\alpha}(^{180}\text{W}) \geq 0.7 \times 10^{18}$ yr at 90% C.L. In addition, new $T_{1/2}$ bounds have been set for α decay of ^{182}W , ^{183}W , ^{184}W , and ^{186}W at the level of $(0.8-1.8) \times 10^{20}$ yr. All these limits are higher than those obtained in previous work [6] and are the most stringent bounds on $T_{1/2}^{\alpha}$ for any α decaying nuclides.

To confirm existence of α activity of ^{180}W , we are preparing measurements with other tungsten containing crystal scintillators: CdWO₄ (whose scintillation characteristics are better than those of currently used crystals), CaWO₄, and ZnWO₄. Observation of the α decay of ^{180}W could be also checked with these crystals as bolometers [22,38] and, apparently, sensitivity of such experiments would be enhanced by using crystals enriched in/depleted of ^{180}W .

ACKNOWLEDGMENTS

The authors would like to thank Dr. Filippo Olmi for the electron microscope measurements of the platinum contaminations in the CdWO₄ crystal and Dr. Mykola Petrenko for the similar measurements performed with the enriched $^{116}\text{CdWO}_4$ crystal.

-
- [1] G. Audi, and A.H. Wapstra, Nucl. Phys. **A595**, 409 (1995).
 [2] W. Porschen and W. Riezler, Z. Naturforsch. A **8a**, 502 (1953); **11a**, 143 (1956).
 [3] K.J.R. Rosman and P.D.P. Taylor, Pure Appl. Chem. **70**, 217 (1998).
 [4] G.B. Beard and W.H. Kelly, Nucl. Phys. **16**, 591 (1960).
 [5] R.D. Macfarlane and T.P. Kohman, Phys. Rev. **121**, 1758 (1961).
 [6] A.Sh. Georgadze *et al.*, Pis'ma Zh. Éksp. Teor. Fiz. **61**, 869 (1995) [JETP Lett. **61**, 882 (1995)].
 [7] B. Buck, A.C. Merchant, and S.M. Perez, J. Phys. G **17**, 1223 (1991).
 [8] D.N. Poenaru and M. Ivascu, J. Physique **44**, 791 (1983).
 [9] P.G. Bizzeti *et al.*, *Proceedings of the 51st Meeting on Nuclear Spectroscopy and Nuclear Structure, Sarov, Russia*, 2001 (Bull. Russ. Acad. Sci., Ser. Phys. **66**, 630 [2002]) in Russian.
 [10] F.A. Danevich *et al.*, Phys. Rev. C **62**, 045501 (2000); P.G. Bizzeti *et al.*, Nucl. Phys. B (Proc. Suppl.) **110**, 389 (2002).
 [11] Yu.G. Zdesenko *et al.*, *Proceedings of the 2nd International Symposium on Underground Physics, Baksan Valley, USSR*, 1987 (Nauka, Moscow, 1988), p. 291.
 [12] F.A. Danevich *et al.*, Phys. Lett. B **344**, 72 (1995).
 [13] T. Fazzini *et al.*, Nucl. Instrum. Methods Phys. Res. A **410**, 213 (1998).
 [14] J.B. Birks, *Theory and Practice of Scintillation Counting* (Pergamon, New York, 1967).
 [15] Computer code GEANT, CERN Program Library, long write-up W5013, CERN, 1994.
 [16] F.A. Danevich *et al.*, Nucl. Phys. **A694**, 375 (2001).
 [17] J.C. Barton and J.A. Edgington, Nucl. Instrum. Methods Phys. Res. A **443**, 277 (2000).
 [18] D.R. Tovey *et al.*, Phys. Lett. B **433**, 150 (1998).
 [19] E. Gatti and F. De Martini, *Nuclear Electronics 2* (IAEA, Vienna, 1962), p. 265.
 [20] F.A. Danevich *et al.*, Phys. At. Nucl. **59**, 1 (1996).
 [21] *Table of Isotopes*, edited by R.B. Firestone *et al.*, 8th ed., (Wiley, New York, 1996).
 [22] A. Alessandrello *et al.*, Nucl. Instrum. Methods Phys. Res. A **344**, 243 (1994); Nucl. Phys. B (Proc. Suppl.) **35**, 394 (1994).
 [23] Particle Data Group, D.E. Groom *et al.*, Eur. Phys. J. C **15**, 1 (2000).
 [24] G.J. Feldman and R.D. Cousins, Phys. Rev. D **57**, 3873 (1998).
 [25] B.C. Grabmaier, IEEE Trans. Nucl. Sci. **NS-31**, No. 1, 372 (1984).
 [26] O.A. Ponkratenko *et al.*, Phys. At. Nucl. **63**, 1282 (2000).
 [27] B. Al-Bataina and J. Janecke, Phys. Rev. C **37**, 1667 (1988).
 [28] National Nuclear Data Center, Brookhaven National Laboratories, New York, www.nndc.bnl.gov/nndc/nudat
 [29] D.N. Poenaru *et al.*, At. Data Nucl. Data Tables **34**, 423 (1986).
 [30] P.O. Froman, Mat. Fys. Medd. K. Dan. Vidensk. Selsk. **1**, No. 3 (1957).
 [31] A.H. Wapstra *et al.*, *Nuclear Spectroscopy Tables* (North-Holland, Amsterdam, 1959).
 [32] R. Taagepera and M. Nurmia, Ann. Acad. Sci. Fenn., Ser. A VI **78**, 1 (1961).
 [33] V.E. Viola, Jr. and G.T. Seaborg, J. Inorg. Nucl. Chem. **28**, 741 (1966).
 [34] K.A. Keller and H. Munzel, Z. Phys. **255**, 419 (1972).
 [35] P. Hornshoj *et al.*, Nucl. Phys. **A230**, 365 (1974).
 [36] B.A. Brown, Phys. Rev. C **46**, 811 (1992).
 [37] P. Moller *et al.*, At. Data Nucl. Data Tables **66**, 131 (1997).
 [38] M. Sisti *et al.*, Nucl. Instrum. Methods Phys. Res. A **444**, 312 (2000).